Volume 1 | Number 1 | Jan 2013 | Pages 1–100

Nanoscale

www.rsc.org/nanoscale

ROYAL SOCIETY OF CHEMISTRY

This is an *Accepted Manuscript*, which has been through the Royal Society of Chemistry peer review process and has been accepted for publication.

Accepted Manuscripts are published online shortly after acceptance, before technical editing, formatting and proof reading. Using this free service, authors can make their results available to the community, in citable form, before we publish the edited article. We will replace this *Accepted Manuscript* with the edited and formatted *Advance Article* as soon as it is available.

You can find more information about *Accepted Manuscripts* in the **Information for Authors**.

Please note that technical editing may introduce minor changes to the text and/or graphics, which may alter content. The journal's standard **Terms & Conditions** and the **Ethical guidelines** still apply. In no event shall the Royal Society of Chemistry be held responsible for any errors or omissions in this *Accepted Manuscript* or any consequences arising from the use of any information it contains.

www.rsc.org/nanoscale

SWNT nano-engineered networks strongly increase charge transport in P3HT

Nicolas Boulanger,[a] Junchun Yu[a] and David R Barbero,[*a]

We demonstrate the formation of arrays of 3D nano-sized networks of interconnected single-wall carbon nanotubes (SWNT) with well defined dimensions in a poly-3-hexylthiophene (P3HT) thin film. These novel nanotube nano-networks produce efficient ohmic charge transport, even at very low nanotube loadings and low voltages. An increase in conductivity between one and two orders of magnitude is observed compared to a random network. The formation of these nano-engineered networks is compatible with large area imprinting and roll to roll processes, which makes it highly desirable for opto-electronic and energy conversion applications using carbon nanotubes.

Carbon nanotubes and polymer composites have recently emerged as a new class of materials with enhanced electrical and/or mechanical properties. In particular, due to their exceptional charge transport, single walled carbon nanotubes are becoming increasingly attractive as additives in semiconducting polymers such as the widely used P3HT for next generation of hybrid and organic photovoltaic devices. [1–6] Recent advances in this field have shown that ultrafast charge transport readily occurs at the interface between SWNTs and P3HT. [7–9] The nanotubes act as highly efficient charge transport pathways, between the P3HT interface and an electrode. However, one important condition for efficient and optimal charge transport is the ability to form a continuous (percolated) network of interconnected tubes between the two interfaces. This aspect has often been overlooked, and several studies have shown that current methods used to form nanotube networks for electronic applications result in random networks with non-optimal charge transport. [10] The methods typically used to form random networks are spin-coating or drop casting from solution, and they result in non-controlled tube interconnection, and in nanotube positioning which is random and not necessarily reproducible (see Fig. 1A). Controlled dispersion of the nanotubes and formation of a continuous (percolated) network of interconnected tubes inside a polymer matrix is important for better charge transport and reproducible electrical properties. We have recently demonstrated a new method which enables the formation of continuous SWNT networks in well ordered nanoscale domains, as shown in Fig. 1B and 1C. [11] The high degree of control provided by this method results in nano-engineered networks with much increased charge transport. In this letter, we demonstrate that such nano-engineered networks strongly enhance charge transport in a P3HT matrix compared to a random network produced by spin-coating over a wide range of nanotube loadings. By varying the concentration of tubes, we show that efficient charge transport occurs at all concentrations, even at very low nanotube loading, much below the percolation threshold (ϕ_c) typically reported in P3HT. Moreover, we find that the charge transport mechanism is very different in the two types of networks, with the nano-networks producing ohmic conduction, and a high conductivity at all concentrations and even at low voltages. A high nanotube loading has often been seen as the most important parameter for efficient charge transport and to obtain high conductivity in nanotube composites. We instead show that the nanoscale interconnectivity of the nanotubes inside the composite is the main factor which influences charge transport, and that high loadings in random networks still produce less efficient conducting pathways compared to nano-engineered networks with much lower concentrations of tubes. Solution processed methods such as spin-coating or drop-casting require much higher concentrations of nanotubes in order to render the composite conductive. This increases materials costs, but it also increases the probability to create bundles which have been shown to decrease charge transport and lower device performance. [12,13]

By increasing the nanoscale interconnectivity of the tubes inside the nano-network, we were able to strongly reduce the concentration required (much below the percolation threshold previously reported) for forming efficient charge transport pathways. Charge transport in P3HT was strongly enhanced at all concentrations compared to a random network produced by traditional solution based methods. The low amount of SWNT used reduces bundling and provides an economical solution for electronic applications because much lower amounts

[a] *Umeå Universitet, Institutionen för Fysik, Linnaeus väg 24, Umeå, Sweden. E-mail: david.barbero@physics.umu.se*
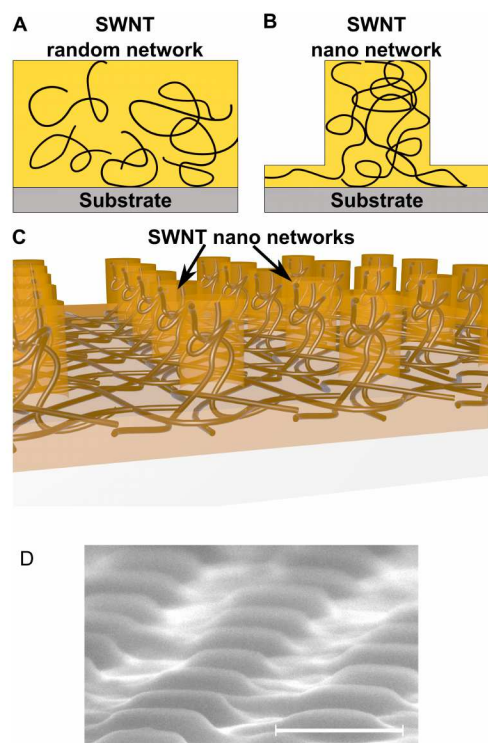
Fig. 1 Network configuration in (a) a random network, (b) a nano-engineered network. The interconnection between nanotubes and the ability to form a continuous path for efficient charge transport is higher in the nano-engineered network. Figure (c) represents a 3D view of an array of nanotube nano-networks, and (d) is a scanning electron micrograph of the nano-networks embedded in P3HT. Scale bar is 400 nm.
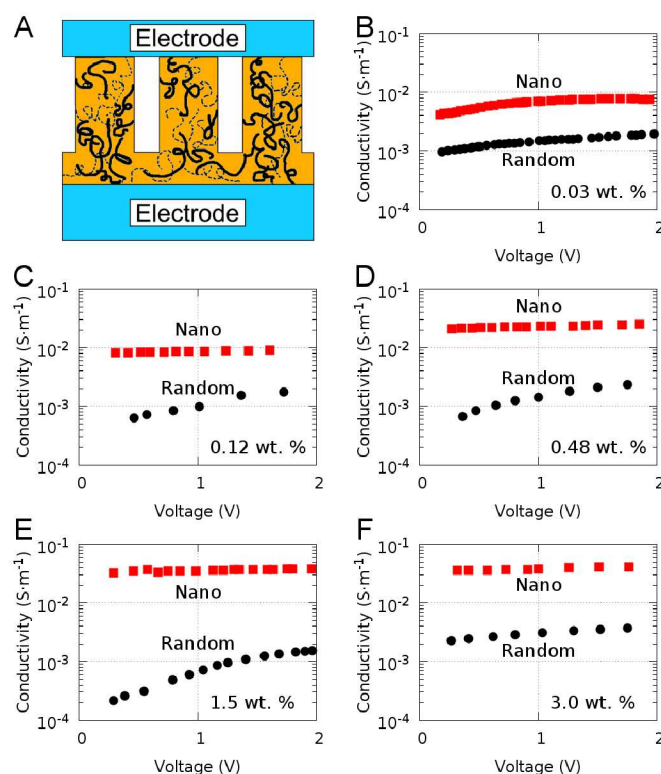

Fig. 2 Schematics of the conductivity measurements in the nano-networks (a). Conductivity of random networks and nano-networks of SWNTs in a P3HT film at various nanotube concentrations: (b) 0.03 wt%, (c) 0.12 wt%, (d) 0.48 wt%, (e) 1.50 wt%, (f) 3.00 wt%.

of expensive nanotubes are necessary. The nanotubes used were mostly semi-conducting (>90%), and were used as purchased from the manufacturer (SouthWest NanoTechnologies) without any purification nor doping. The nanotubes were dispersed in ortho-dichlorobenzene (o-DCB), ultrasonicated for 60 minutes. The SWNT nano-networks were produced by spin-coating a thin layer of nanotubes and an additional layer of regio-regular P3HT (M_w=24 000 g·mol^{-1}) onto a doped conductive silicon substrate (resistivity 0.002–0.005 Ω·cm). This configuration was then nanoimprinted with a soft mold made of polydimethylsiloxane (PDMS) with 400 nm wide and 350 nm high pillars at 200°C and 20 bar.[14] The random networks were produced by spin-coating a thin-film from a solution of the P3HT and nanotubes mixed together. Films with different nanotube concentrations ranging from ≈100 times below the reported percolation threshold (ϕ_c ≈2–3 wt.%) in P3HT to 3 wt.% were produced by the methods described above.[15] Figure 1 shows the nanoscale network organization in (a) a typical random network, and (b) a nano-patterned network inside a thin film. In the random network, the tubes are not optimally interconnected and only a small portion contributes to charge transport across the film thickness. By contrast, the formation of nano-patterned networks results in much more efficient percolation between tubes and results in a strong increase in electrical conduction, even at low loadings. The concentrations of SWNTs used were ranging from ≈0.03 wt.% to ≈3 wt.%, and the details of the samples prepared and measured here indicated in Table 1.

Figure 2 shows the conductivity of the SWNT/P3HT composite films with either a random network, or with a nano-engineered network of nanotubes as a function of the voltage applied between the top and the bottom of the film. The voltage was varied with a small step of 0.1V, and the current flowing across the film (from top to bottom) was measured for each applied voltage. In the case of the nanopatterns, the current was measured between the top and the bottom of the pattern. Measurements were repeated up to 10 times in each location, and in 3 different locations on each sample, and showed good reproducibility. The conductivity σ was calculated for each
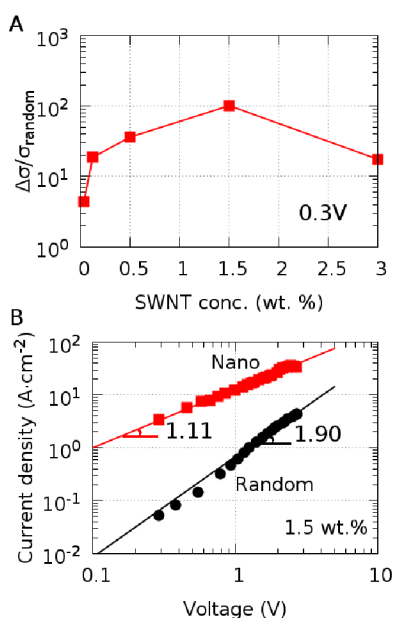
Nanoscale Accepted Manuscript

Fig. 3 Electrical characteristics of the networks. (a) Increase in conductivity in the nano-network compared to the random network as a function of nanotube concentrations at low voltage (0.3 V). (b) Typical current density – voltage characteristics of random and nano-networks, showing ohmic conduction in the nano-network ($a \approx 1.0$) and non-ohmic conduction in the random network.

applied voltage as:

$$\sigma = \frac{I}{V} \frac{t}{A} \qquad (1)$$

where I is the measured current, V is the applied voltage, t the sample thickness measured by AFM and A the sample/electrode contact area. The data in Figure 2 shows that the conductivity in the random network stays nearly the same (and nearly identical to that of pure P3HT) at all concentrations below ≈ 3 wt%, which is close to the percolation threshold previously reported in this system. However, the nano-network is consistently much more conductive, even at very low nanotube loading where $\sigma_{nano} \approx 5$ times higher than σ_{random}, which indicates more efficient charge transport and much better interconnectivity between tubes in the nano-networks. At ≈ 3 wt%, the conductivity in the nano-network reaches $\sigma \approx 5.10^{-2}$ S·m^{-1}, which is more than 10 times higher than in the random network. Figure 3 shows the increase in conductivity (in number of times increased) of (σ_{nano} - σ_{random}) divided by σ_{random} as a function of the concentration of nanotubes at 0.3 V applied voltage. At all concentrations below 3.0 wt%, the random network did not form an efficient network for charge transport, which is consistent with previously published results. However, the nano-network is already 5 times more conductive at the lowest concentration of 0.03 wt%, and becomes more and more conductive with higher loadings, reaching a peak of

≈ 100 times more conductive than the random network at a concentration of ≈ 1.5 wt%. Close to the percolation threshold of the random network (≈ 3.0 wt%), σ_{random} increases as expected but the nano-network still remains nearly 20 times more conductive. Moreover, it can be noticed in Figure 2 that the conductivity in the nano-network is also nearly constant from low to high applied voltage, whereas the conductivity in the random network is much lower at low voltage, and it increases at higher voltage. This shows that the nano-engineering of the tubes network also provides much better charge transport at low voltage (≈ 0.2–1.0 V), which is advantageous for certain applications, e.g. organic and hybrid photovoltaics.[16]

Table 1 Exponent a of the slopes of the log-log of J–V for the various networks at different SWNT concentrations.

SWNT conc. (wt.%)	Nano-network	Random network
0.03	1.11	1.37
0.12	1.02	1.66
0.48	1.05	1.64
1.50	1.11	1.90
3.00	1.09	1.33

The current density (J)–voltage (V) characteristics for the random and the nano networks are shown in Figure 3 b. The data was fitted with a power law: $J = b * V^a$ where J is the measured current density and V is the applied voltage. In a log–log plot, as shown in Figure 3, the exponent a gives the slope of the relationship between J and V and is reported in Table 1 at all concentrations.[17] A very different behavior is observed between the typical random network, and the nano-engineered network. The nano-networks display an exponent $a \approx 1.02$–1.11 at all concentrations, which is characteristic of ohmic conduction. By contrast, conduction in the random network is clearly non-ohmic, with values of the exponent $a \approx 1.33$–1.90. Conduction in pure P3HT has been described as space-charge limited with a quadratic variation of the current density with voltage (a=2). The values of a measured in the random network indicate a conduction which is partially space-charge limited, and which is likely due to poor interconnection between tubes inside the film which leads to non-ohmic charge transport, and much lower conductivities compared to the nano-network. Ohmic conduction in the nanoscale networks can be explained by the formation of continuous paths with highly interconnected tubes which bridge the gap between the top and the bottom of the film. During the formation of the nano-networks, the nanotubes are pushed into the cavities of the patterned mold by shear forces acting on the SWNT/polymer composite. The nanotubes were first oriented in the plane of the film, in a quasi-2D geometry (film's
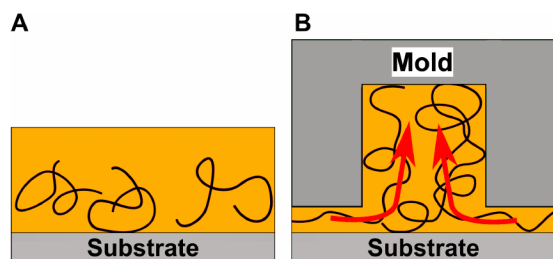
Fig. 4 Mechanism of nano-network formation. Figure (a) represents a two-layer composite film with a nanotubes and polymer film. Figure (b) shows formation of the nano-network, where the arrows indicate flow of nanotubes inside the mold's cavity to form a pathway for charge transport from top to the bottom of the pattern.

thickness $\approx 20\,$nm). When the second layer of pure P3HT is spun on top of the nanotubes, the film's conductivity remains identical to that of pure P3HT ($\sigma \approx 10^{-3}$ S·m^{-1}). After formation of the nano-networks in this composite film, the conductivity increases by more than one order of magnitude, to $\sigma \approx 10^{-2}$ S·m^{-1} at a low SWNT concentration of $\approx$0.03 wt%.

This 10 fold increase in conductivity in the nano-networks clearly shows that the nanotubes are reoriented from a planar orientation to a more vertical orientation during nano-network formation. This re-orientation of the tubes can be explained by the flow of the composite inside the mold which fills the cavity from the bottom to its top as shown in Figure 4.[18-21] The nanotubes are therefore dragged with the flow of the liquid composite and form a conducting path from top to bottom of the patterns. Considering the patterns dimensions ($\approx$400 nm diameter and $\approx$300 nm high), it is even possible that single nanotubes form a direct conducting path by bridging the whole film thickness. Indeed, the nanotube average length is $\approx$700 nm, which is longer than the thickness of the nanopatterned film ($\approx$400 nm). The film thickness in the random network is $\approx$120 nm, and tube bridging would be expected here too, but it is clearly not observed from the low conductivity measured in the random networks. This shows that efficient pathways and contacts are formed from top to bottom of the film during flow of the tubes inside the nano-network, which leads to a different architecture with a higher degree of interconnection between tubes compared to a typical random network formed by spin-coating.

In conclusion, we have shown that the formation of an array of well-defined nano-scale networks of nanotubes produces efficient charge transport inside a P3HT film, with an increase in conductivity by as much as $\approx$100 times compared to a traditional random network. The nano-networks showed ohmic conduction at all concentrations, and a nearly constant conductivity at all applied voltages, including low voltages ($<0.5\,$V). We believe these novel nano-engineered networks should be very appealing for hybrid and carbon based energy conversion devices such as photovoltaic solar cells.

Acknowledgements

References

1 M. W. Rowell, M. A. Topinka, M. D. McGehee, H.-J. Prall, G. Dennler, N. S. Sariciftci, L. Hu and G. Gruner, *Appl. Phys. Lett.*, 2006, **88**, 233506.
2 F. S. Kim, G. Ren and S. A. Jenekhe, *Chem. Mater.*, 2011, **23**, 682–732.
3 E. Kymakis, M. M. Stylianakis, G. D. Spyropoulos, E. Stratakis, E. Koudoumas and C. Fotakis, *Sol. Energy Mater. Sol. Cells*, 2012, **96**, 298–301.
4 C. Niu, *MRS Bulletin*, 2011, **36**, 766–773.
5 Z. Yang, T. Chen, R. He, G. Guan, H. Li, L. Qiu and H. Peng, *Adv. Mater.*, 2011, **23**, 5436–5439.
6 H. Derbal-Habak, C. Bergeret, J. Cousseau and J. M. Nunzi, *Sol. Energy Mater. Sol. Cells*, 2011, **95**, S53–S56.
7 D. J. Bindl, N. S. Safron and M. S. Arnold, *ACS Nano*, 2010, **4**, 5657–5664.
8 M. Bernardi, M. Giulianini and J. Grossman, *ACS Nano*, 2010, **4**, 6599–6606.
9 S. D. Stranks, C. Weisspfennig, P. Parkinson, M. B. Johnston, L. M. Herz and R. J. Nicholas, *Nano Lett.*, 2011, **11**, 66–72.
10 J. Di, Z. Yong, X. Zheng, B. Sun and Q. Li, *Small*, 2013, **9**, 1367–1372.
11 D. R. Barbero, N. Boulanger, M. Ramstedt and J. Yu, *Adv. Mater.*, 2014, DOI: 10.1002/adma.201305843.
12 J. Yang, N. Yang, D. Zhang, X. Wang, Y. Li and Y. Li, *J. Phys. Chem. C*, 2012, **116**, 22028–22035.
13 P. Luo, H. Wu and M. Morbidelli, *Carbon*, 2014, **68**, 610–618.
14 D. R. Barbero, M. S. M. Saifullah, P. Hoffmann, H. J. Mathieu, D. Anderson, G. A. C. Jones, M. E. Welland and U. Steiner, *Adv. Funct. Mater.*, 2007, **17**, 2419–2425.
15 I. Singh, P. Bhatnagar, P. Mathur, I. Kaur, L. Bharadwaj and R. Pandey, *Carbon*, 2008, **46**, 1141–1144.
16 S. A. Gevorgyan, O. Zubillaga, J. M. V. de Seoane, M. Machado, E. A. Parlak, N. Tore, E. Voroshazi, T. Aernouts, H. Mllejans, G. Bardizza, N. Taylor, W. Verhees, J. M. Kroon, P. Morvillo, C. Minarini, F. Roca, F. A. Castro, S. Cros, B. Lechhne, J. F. Trigo, C. Guilln, J. Herrero, B. Zimmermann, S. B. Sapkota, C. Veit, U. Wrfel, P. S. Tuladhar, J. R. Durrant, S. Winter, S. Rousu, M. Vlimki, V. Hinrichs, S. R. Cowan, D. C. Olson, P. Sommer-Larsen and F. C. Krebs, *Renewable Energy*, 2014, **63**, 376–387.
17 Z. Chiguvare, J. Parisi and V. Dyakonov, *J. Appl. Phys.*, 2003, **94**, 2440–2448.
18 L. J. Heyderman, H. Schift, C. David, J. Gobrecht and T. Schweizer, *Microelectron. Eng.*, 2000, **54**, 229–245.
19 Y. Xu, F. Tsumori, T. Toyooka, H. Kotera and H. Miura, *Jpn. J. Appl. Phys.*, 2011, **50**, 06GK11.
20 D. Jun, W. Zhengying, L. Shize and T. Yiping, *Microsyst. Technol.*, 2013, **19**, 1229–1238.
21 L. Peng, Y. Deng, P. Yi and X. Lai, *J. Micromech. Microeng.*, 2014, **24**, 013001.